



Universiteit  
Leiden  
The Netherlands

## **Optimal photosensitizers for photodynamic therapy : the preparation and characterization of novel photosensitizers derived from mesoporphyrin**

Haas, H.H.S. van der

### **Citation**

Haas, H. H. S. van der. (2006, June 14). *Optimal photosensitizers for photodynamic therapy : the preparation and characterization of novel photosensitizers derived from mesoporphyrin*. Department Bio-Organic Photochemistry, Faculty of Mathematics and Natural Sciences, Leiden University. Retrieved from <https://hdl.handle.net/1887/11405>

Version: Corrected Publisher's Version

License: [Licence agreement concerning inclusion of doctoral thesis in the Institutional Repository of the University of Leiden](#)

Downloaded from: <https://hdl.handle.net/1887/11405>

**Note:** To cite this publication please use the final published version (if applicable).

# Chapter 5

## General Discussion and Prospects

## § 5.1 General discussion

In chapter two the simple preparation of six novel quino[4,4a,5,6]-annulated porphyrin derivatives is described. Their structural assignment is based on  $^1\text{H-NMR}$ -,  $^{13}\text{C-NMR}$ - and mass spectroscopy. The formation of the quinoline system starts with the attack of a proton from trichloroacetic acid on the nitrogen of the acrylonitrile side-chain (see fig 5.1 and scheme 2.3 of chapter 2). The resulting positively charged carbon of the protonated cyano-group in the Z-isomer attacks a carbon atom of the neighboring pyrrole ring B that via subsequent reactions forms besides an appending benzene ring also a pyridine ring under expulsion of a methyl group and oxidation.

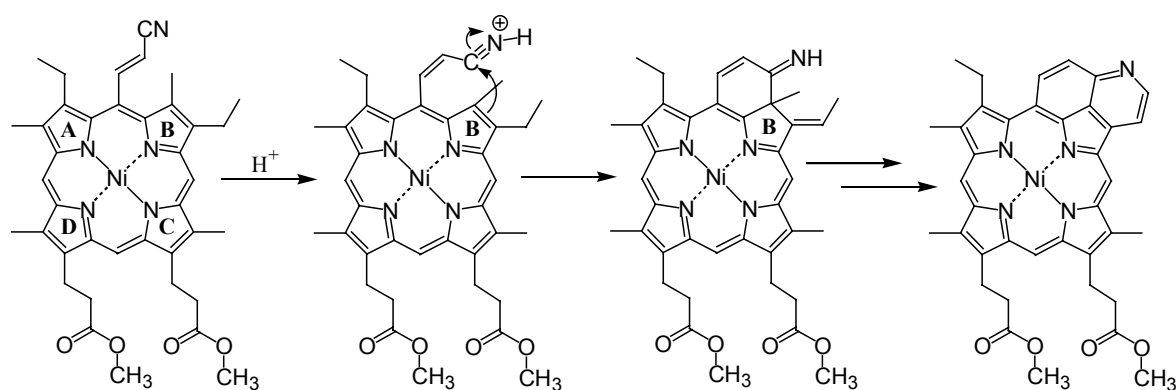


**Figure 5.1**, plausible reaction mechanism for the formation of peri-condensed quino fused porphyrins.

It was observed that at the temperature at which these reactions were carried out E / Z isomerization takes place. With  $^1\text{H NMR}$  the presence of the Z-isomer could be directly observed. In the end during this one-pot reaction a porphyrin with a fused quinolin ring system is formed. 5-(2'-cyanovinyl)mesoporphyrin only gives the product of attack on the B-ring and not the A-ring because in the latter case no stable aromatic peri-condensed quinoline system can be formed. Presumably the alternative attack on the A-ring will lead to unidentified side products, which is a possible explanation for the low yield of the novel products.

After the reactions of chapter 2 and 3 had been published we became aware of work reported on the acetic acid treatment of free base 5-(2-cyanovinyl)porphyrins. These systems gave purpurins (see figure 5.2) with absorption maximum at 694 nm.<sup>[1]</sup>

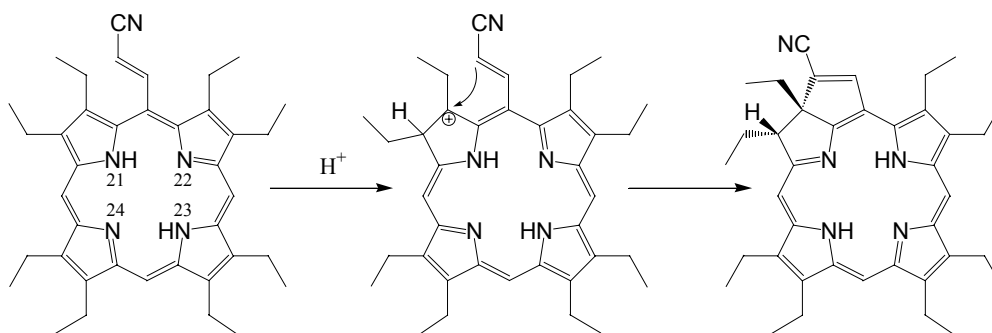


**Figure 5.2.** Cyclization of free base meso-(2-cyanovinyl)octaethylporphyrin under acidic conditions.

This latter reaction of the acrylonitrile function is very similar to the one described by R. B. Woodward et. al. for the intermediate with the acryl ester function during the chlorophyll total synthesis (see chapter 2, figure 1).<sup>[2]</sup> The difference with the Ni<sup>2+</sup>-porphyrins may be related to the fact that the presence of two central hydrogen ions breaks the symmetry of the system. E.g. the two protons are either attached to the nitrogen atoms 21 and 23 or to 22 and 24. These two tautomers are in thermodynamic equilibrium at room temperature. Two electron-rich pyrrole rings and two electron poor aza-rings are present, which is not the case in the Ni-porphyrin system where all rings are electronically equal. One can now imagine that there will be an easy protonation of a  $\beta$ -carbon at a pyrrole-ring leading to the formation of a  $sp^3$  center and a carbenium ion center on the adjacent  $sp^2$  carbon (Figure 5.2). The latter can attack carbon 2 of the appending acrylonitrile part in an intramolecular process. Subsequent loss of the proton of the resulting intermediate carbenium ion leads to the purpurins. The second step is analogous to the reaction on the appending acrylonitrile group by an external carbenium ion as described in the third chapter. In the third chapter we describe the novel 2'-cyano-8'-formyl-N'-methyl-1',1a',5a',6'-tetrahydroacrido[4,5,5a,6-bcd]annulated 2,3-dihydromesoporphyrin dimethylester.

In both cases the Ni<sup>2+</sup> can be removed and free base quino[4,4a,5,6-efg]-8-deethyl-7-demethylmesoporphyrin dimethylester and the free base of 2'-cyano-8'-formyl-N'-methyl-1',1a',5a',6'-tetrahydroacrido[4,5,5a,6-bcd]-annulated 2,3-dihydromesoporphyrin dimethylester are obtained. These systems have strong absorption at 681 nm and 688 nm respectively, in the far-red region of the visible spectrum. These systems have all properties to serve as an efficient photosensitizer for photodynamic therapy. The water solubility of the two different systems was improved by saponification of the ester

functions into the carboxylates by reaction with sodium hydroxide in a mixture of methanol and water (9:1). The products were purified with an acidic ion exchange column and followed by one over a basic ion exchange column.

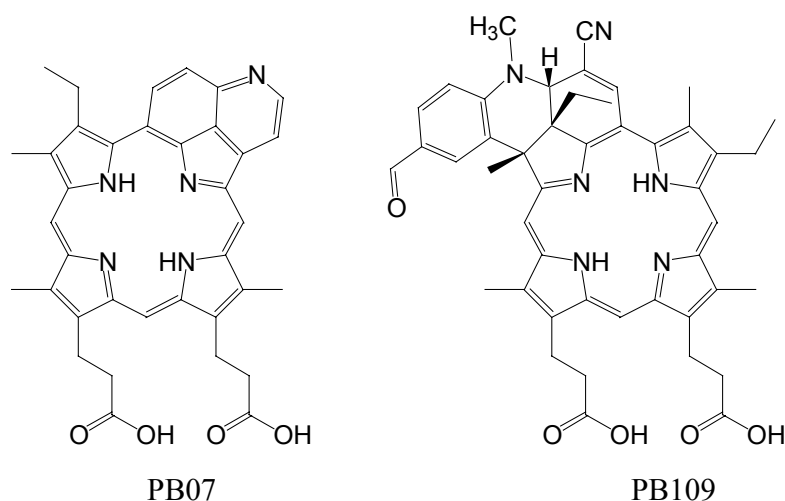


**Figure 5.3,** Structures of the mesoporphyrin based photosensitizers PB07 and PB109 currently under investigation for application in photodynamic therapy.

The  $^1\text{H}$  NMR-spectra of both products were fully in agreement with the structures as was established by comparison with the  $^1\text{H}$ -NMR spectra of the corresponding methyl esters. The resulting acids are named PB07 and PB109 for easy communication and their structures are depicted in figure 5.3.

In order to obtain a product with  $\lambda_{\text{max}}$  in the near infrared part of the visible spectrum we treated the product depicted in figure 5.1 with benzyl iodide, which led to the benzylation product with a  $\lambda_{\text{max}}$  at 755 nm.

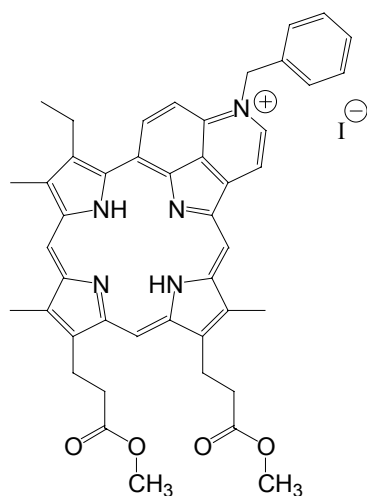


**Figure 5.4,** Structure of the product obtained when the quinoline nitrogen of the quino annulated porphyrin depicted in figure 5.1 is quaternized with benzyl iodide.

The structure of this compound is given in figure 5.4. For the further research we have focussed on the preclinical trials of PB07 and PB109 before starting a research based on finding the optimal alkylgroup forming the N-alkylquinolinium derivative.

In chapter three is also discussed that treatment of the 5-(2'-cyanovinyl)mesoporphyrin dimethylester with the Vilsmeier reagent of dimethylformamide leads to a mixture of two quino-annulated mesoporphyrin derivatives, which could thus far not be separated into the two pure forms. In this case after the initial attack of the Vilsmeier reagent at the nitrogen of the acrylonitrile function the positively charged carbon of the cyano group attacks either the carbon atom of the appending pyrrole ring A or that of pyrrole ring B. In the earlier mentioned cases only one quino-annulated product was obtained. In the case of the Vilsmeier reaction with dimethylformamide the solution might be found in the replacement of the two ethyl groups of 5-(2-cyanovinyl)mesoporphyrin into two methyl groups. This leads to a symmetrical situation such that during the Vilsmeier reaction only one product will be formed. In this case no uncontrollable oxidation by oxygen from air is necessary anymore. This procedure may lead to more quino[4,4a,5,6]-annulated porphyrins in higher yield.

A similar approach may also work in the case of the reaction with the Vilsmeier reagent prepared from aromatic formamides. Further the number of possible Vilsmeier reagent is very large, which means that many more quino[4,4a,5,6]-annulated porphyrins and 2'-cyano-8'-formyl-N-methyl-1',1a',5a',6'-tetrahydroacrido[4,5,5a,6]-annulated 2,3-dihydroporphyrins can now in principle be prepared without problems. Having an extended library of such compounds in hand will allow a selection of systems that have even better properties as a basis for photodynamic therapy than the two systems now under investigation.

In chapter 4 an  $^1\text{H-NMR}$  study of free base and zinc(II) complexes derived from mesoporphyrin, protoporphyrin and deuteroporphyrin with appending functionalized ethylamide groups attached to the propionic side chains in ring C and D is presented.

Especially the alkoxygroups attached to carbon atom 2 of the ethyl amide side chains show large upfield shifts. Also the chemical shift difference of the diastereotopic ethoxy and 2-propoxy fragments is larger than in the analogous model system. These facts can be explained by assuming that the side chains are in a dynamic equilibrium in close proximity to the A and B rings of the porphyrin system. This research clearly shows that the porphyrin ring and its aliphatic side chains prefer to have close contact.

## § 5.2 Biological properties of the new photosensitizers

The initial biological tests of the systems have been reported in chapters 2 and 3. The investigations described in this thesis were carried out with financial support from (STW) in which the firm PhotoBioChem has extended the biological tests in preclinical evaluations. A group of the Ecole Polytechnique Fédérale de Lausanne has reported on the results of PB07 and PB109 on the chick's chorioallantoic membranes (CAM) as *in vivo* model for photodynamic agents for blood vessel closure in age related macular degeneration (AMD).<sup>[3]</sup> AMD is a serious disease that strikes older people and leads to loss of light sensitivity in the central part in the retina and may lead to total blindness. In ageing populations the occurrence of this affliction increases dramatically. The conclusion is that PB07 and PB109 do not rapidly leak out from the blood vasculature after intravenous injection. Therefore it has been concluded that the risk to damage normal neighboring structures such as pigment epithelium or choriocapillaries in the case of photodynamic therapy on AMD could be strongly decreased. The leakage profile of PB07 and PB109 observed in the model is a significant improvement over Visudyne<sup>®</sup>. With respect to the therapeutic effect, the vascular occlusion observed after PDT with both photosensitizers are quite encouraging for the treatment of diseases associated with angiogenesis, their potency being comparable to that of the reference photosensitizer, Visudyne<sup>®</sup>.

Similarly the antitumor PDT efficacy and skin photosensitivity in the mouse by PB07 and PB109 has been tested by the Centre for Photobiology and Photodynamic therapy at the University of Leeds<sup>[4]</sup>. Following *in vivo* administration to CBA/Gy mice bearing a subcutaneous CaNT tumour, both PB07 and PB109 show maximum antitumour PDT efficacy at a drug to light interval of 2 minutes, and negligible activity by 3h drug to light interval. Photodynamic activity is broadly of the same order of magnitude as that of Photofrin<sup>®</sup> (PHP), but with a 2.5 fold advantage for PB07 and PB109, when compared with PHP at the optimal drug to light intervals. Both PB07 and PB109 cause PDT induced-damage to normal internal tissues. Whilst this is sometimes observed in this model as a result of the close proximity of the subcutaneous tumour to internal organs in the mouse, in some animals with PB07 and PB09, this damage was severe and normal tissue damage was still observed with PB109 at 3h drug to light interval, despite the fact that tumour necrosis was negligible at this time point. For comparative purposes, at equitoxic doses, the average level of normal tissue damage was similar to that caused by PHP. PB07 predominantly caused damage to the quadriceps muscle while PB109, in common with PHP,

predominantly affected the liver. The incidence of eschar formation in the skin overlying the tumour after PDT was lower for PB07 and PB109 compared to PHP at equitoxic doses. No skin photosensitivity (as measured by change in ear thickness following solar simulation) was observed 24h or 2 weeks after *in vitro* administration of PB07 or PB109 to CBA/Gy mice at the therapeutic dose (3.34  $\mu\text{mol/kg}$ ). For both PB07 and PB109, 40% of the mice developed eschars on their tails above the point of injection approximately 1 week post dose. In contrast, high levels of skin photosensitivity were observed when PHP was administered at the therapeutic dose (8.35  $\mu\text{mol/kg}$ ). PB07 at the maximum injectable dose of 13.3  $\mu\text{mol/kg}$  also did not cause any skin photosensitivity, however skin photosensitivity was observed 24h after administration of PB109 at the maximum injectable dose of 5.2  $\mu\text{mol/kg}$ .

For development of new PDT photosensitisers, it is desirable to prove advantages over currently approved compounds (Photofrin<sup>®</sup> and Foscan<sup>®</sup>). This demands shorter drug to light interval, less skin photosensitivity and greater selectivity between tumour and normal tissue. This study has demonstrated that both PB07 and PB109 have the potential to show reduced skin photosensitivity and reduced drug to light interval compared with Photofrin<sup>®</sup> and Foscan<sup>®</sup>, but the study has not clearly demonstrated greater selectivity.

### § 5.3 References

- [1] B. C. Robinson, and A. R. Morgan, *Proc. SPIE* **1996** 2675, 191-199.
- [2] R. B. Woodward, G. L. Closs, E. leGoff, W. A. Ayer, H. Dutler, W. Leimgruber, J. M. Beaton, J. Hannah, W. Lwowski, F. Bickelhaupt, F. P. Hauck, J. Sauer, R. Bonnett, S. Ito, Z. Valenta, P. Buchschacher, A. Langeman and H. Volz, *J. Am. Chem. Soc.* **1960**, 82, 3800-3802. For a description in full experimental detail: *Tetrahedron*, **1990**, 46, 7555-7659.
- [3] E. Debeve, B. Pegaz, G. Wagnières, J.-P. Ballini and H. van den Bergh, Internal report of PhotoBioChem: Pre-clinical Evaluation of PhotoBioChem's Agents PB07 and PB109 on the CAM model as blood vessel closure in age-related Macular Degeneration., September 2005, Ecole Polytechnique Fédérale de Lausanne (EPFL), Switzerland.
- [4] Internal report of PhotoBioChem, august 2005, Project PPA-PB-01, Anti-tumour PDT efficacy and skin photosensitivity in the mouse, The Centre for Photobiology and Photodynamic Therapy, University of Leeds, United Kingdom.



